J. Fluid Mech. (1981), *vol.* 112, *pp.* 363–377
Printed in Great Britain

Bend theory of river meanders. Part 1. Linear development

By SYUNSUKE IKEDA,
Department of Foundation Engineering, Saitama University, Saitama, Japan
GARY PARKER
St Anthony Falls Hydraulic Laboratory, University of Minnesota, Minneapolis, Minnesota, 55414, USA
AND KENJI SAWAI
Disaster Prevention Research Institute, Kyoto University, Uji, Japan

(Received 31 December 1979 and in revised form 26 June 1981)

Instability of the alternate-bar type in straight channels has long been identified as the cause of fluvial meandering. The condition of inerodible sidewalls, however, does not allow a meandering channel to develop. Herein a stability analysis of a sinuous channel with erodible banks allows for delineation of a 'bend' instability that does not occur in straight channels, and differs from the alternate-bar instability.

In the case of alluvial meanders, the two mechanisms are shown to operate at similar characteristic wavelengths. This provides a rationale for the continuous evolution of alternate bars into true bends such that each bend contains one alternate bar.

The same bend instability applies to incised meanders. A mechanism for incised alternate bars which differs from that for the alluvial case appears to operate at different characteristic wavelengths than that of bend instability. Analysis of data suggests that meandering in supraglacial meltwater streams is primarily due to the alternate bar mechanism, whereas the meandering of rills incised in cohesive material and of caves is likely due to the bend mechanism.

The meander wavelength of incised reaches of meandering streams is often longer than that of adjacent alluvial reaches. An explanation is offered in terms of bend instability.

1. Introduction

Stability theories of fluvial meandering have proliferated since the original work of Hansen (1967) and Callander (1969), and include the work of Adachi (1967), Hayashi (1970), Sukegawa (1970), Engelund & Skovgaard (1973), Parker (1975, 1976), Ponce & Mahmood (1976), Hayashi & Ozaki (1976), and Fredsoe (1978). Parker (1975) treated the incisional case, for which only erosion occurs. Examples of this type are bedrock meanders, meltwater streams on ice (Leopold, Wolman & Miller 1964), cave meanders (Smart 1977), and badland rills (Ashida & Sawai 1977). The other analyses treat the more familiar case of alluvial meanders.

All the above analyses are, however, unsatisfactory due to the fact that bank deformation is not allowed. They treat only the formation of alternate bars between straight, non-erodible banks; the flow may wind about the bars, but the channel does

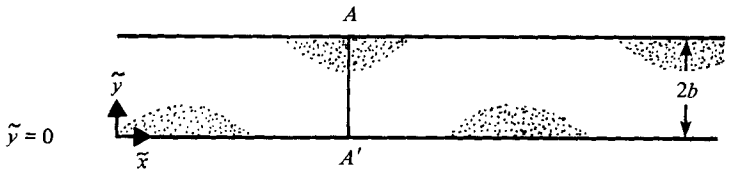

FIGURE 1. Straight channel with inerodible banks and erodible bed containing submerged alternate bars.

not meander (figure 1). It has been implicitly assumed that the concentration of flow against the bank opposite each bar would induce bank erosion, leading to a truly meandering channel with an initial wavelength close to that of the bars from which it derives. While this has been observed experimentally, it has never been given a mechanistic justification.

A first step in this direction was taken by Ikeda, Hino & Kikkawa (1976) (an account in English is given by Ikeda (1978)). Employing Engelund's (1974) second approximation to flow in meander bends, they heuristically explored the consequences of relaxing the restraint of fixed sidewalls. Neither a stability analysis nor a relation governing bank erosion was presented, however, and as a result several of the results are, in retrospect, incorrect (e.g. Ashida & Sawai 1977).

In the present analysis the heuristic model of Ikeda *et al.* is used to develop a formal stability theory of channels with sinuous banks. Bank erosion is described, and the stability criterion is in terms of the growth-rate of lateral bend amplitude. This aspect suggests the parlance of 'bend' theory, as opposed to the previously quoted 'bar' theories. The bend theory is applied to both the alluvial and incised cases. The linear theory herein yields a relation for initial characteristic bend wavelength that rather differs from that of Ikeda *et al.* and shows much better agreement with data. A comparison with the predictions of one of the 'bar' theories indicates that, for alluvial streams, bar and bend instabilities operate at similar wavelengths when sinuosity is not too large.

In part 2 of this work (Parker, Sawai & Ikeda 1982) nonlinear deformation of finite-amplitude bends is considered.

2. Equations of fluid motion

The analysis of bend instability is based on the St Venant equations of shallow water flow in a sinuous, slowly migrating channel with normal half-width b, centreline located at $\tilde{y} = \tilde{y}(\tilde{x}, \tilde{t})$, and centreline curvature $\tilde{\mathscr{C}}(\tilde{x}, \tilde{t})$ (figure 2). The following assumptions are made.

(1) Normal channel width is constant. This is suggested by the observation that many meandering alluvial streams maintain roughly constant width even while actively migrating. Alluvial streams accomplish this by balancing erosion at one bank with deposition at the opposite bank. Vertical and lateral incision tend to balance in incised streams, leading to the same effect.

(2) The centreline radius of curvature at the bend apex r_0 is large in the sense that $\nu = b/r_0 \ll 1$.

(3) The classical quasi-steady assumption holds.

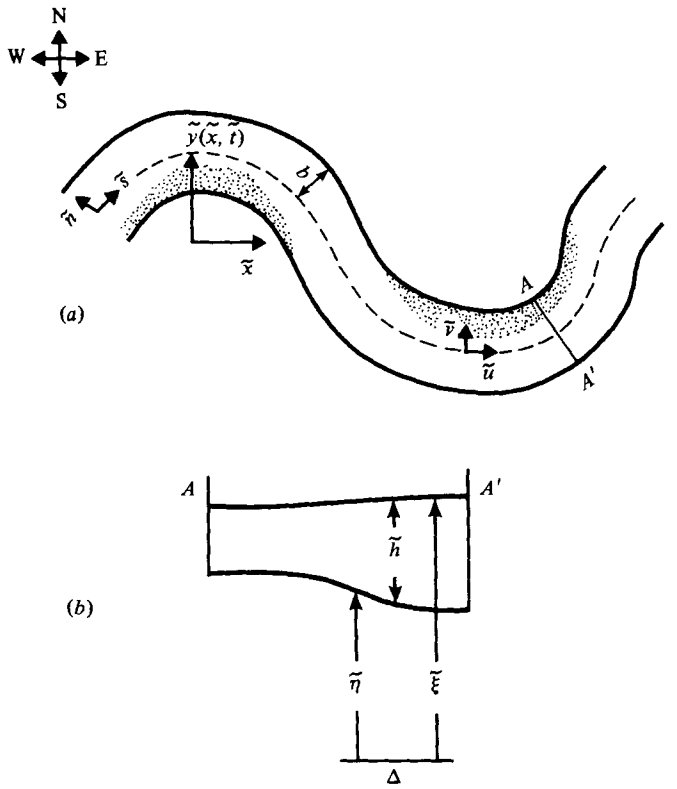

FIGURE 2. Definition diagrams. (*a*) Meandering channel with erodible banks. The hatching indicates submerged point bars. (*b*) Cross-section A–A' of the meandering channel.

The equations of motion for a sinuous channel can then be written as

$$\tilde{u}\frac{\partial \tilde{u}}{\partial \tilde{s}} + \tilde{v}\frac{\partial \tilde{u}}{\partial \tilde{n}} + \tilde{\mathscr{C}}\tilde{u}\tilde{v} = -g\frac{\partial \tilde{\xi}}{\partial \tilde{s}} - \frac{\tilde{\tau}_s}{\rho \tilde{h}}, \tag{1a}$$

$$\tilde{u}\frac{\partial \tilde{v}}{\partial \tilde{s}} + \tilde{v}\frac{\partial \tilde{v}}{\partial \tilde{n}} - \tilde{\mathscr{C}}\tilde{u}^2 = -g\frac{\partial \tilde{\xi}}{\partial \tilde{n}} - \frac{\tilde{\tau}_n}{\rho \tilde{h}}, \tag{1b}$$

$$\tilde{\mathscr{C}}\tilde{v}\tilde{h} + \frac{\partial \tilde{v}\tilde{h}}{\partial \tilde{n}} + \frac{\partial \tilde{u}\tilde{h}}{\partial \tilde{s}} = 0. \tag{1c}$$

In the above ρ is water density; $\tilde{u}$ and $\tilde{v}$ are depth-averaged velocity components in the $\tilde{s}$ and $\tilde{n}$ directions respectively (figure 2); g is the acceleration of gravity; $\tilde{\tau}_s$ and $\tilde{\tau}_n$ are the bed stresses; $\tilde{h}$ is local depth; and $\tilde{\xi}$ is water-surface elevation. Also $\tilde{h} = \tilde{\xi} - \tilde{\eta}$, where $\tilde{\eta}$ is bed elevation. The tilde is used to denote dimensional variables.

Bed stresses are evaluated with the use of a friction factor C_f;

$$\tilde{\tau}_s = \rho C_f \tilde{\mathscr{U}}\tilde{u}, \quad \tilde{\tau}_n = \rho C_f \tilde{\mathscr{U}}\tilde{v},$$

where $\tilde{\mathscr{U}} = (\tilde{u}^2 + \tilde{v}^2)^{\frac{1}{2}}$. For the present analysis the crude assumption of constant C_f is made.

These equations can be directly linearized for small perturbations, so as to provide forms appropriate for the present linear analysis. However, a somewhat more intricate

procedure is utilized herein so as to facilitate the nonlinear analysis of Part 2. The assumption of small ν is used to carry out an informal expansion in this parameter. Only terms up to $O(\nu^2)$, corresponding to Engelund's (1974) second approximation, are retained here and in Part 2, and the $O(\nu^3)$ dynamic nonlinearities (so termed because they occur in the equations of motion) are dropped.

However certain geometric nonlinearities associated with the transformation from intrinsic to Cartesian co-ordinates also arise. They are scaled by the parameter $\delta_0 = 2\pi y_0/\lambda$, where y_0 is initial bend amplitude and λ is bend wavelength. The present linear analysis is performed for infinitesimal bends in the sense that $\delta_0 \ll 1$; however in Part 2 $O(\delta_0^3)$ geometric nonlinearities are retained, allowing for a treatment of finite-amplitude bends. The conditions under which neglect of $O(\nu^3)$ terms but retention of $O(\delta_0^3)$ terms is valid are discussed in Part 2.

Let U, H, and I be reach-averaged (e.g. over one wavelength) tangential velocity, depth, and down-channel energy slope. Also let ξ_0 and η_0 denote running reach-averaged water-surface bed elevations, given by $\xi_0 = \xi_r - I\tilde{s}$ and $\eta_0 = \eta_r - I\tilde{s}$, where η_r and ξ_r are reference elevations for which $H = \xi_r - \eta_r$. Local flow is defined in terms of each of these unperturbed parameters plus a primed quantity denoting a perturbation induced by channel curvature; $\tilde{u} = U + u'$, $\tilde{v} = v'$, $\tilde{h} = H + h'$, $\tilde{\xi} = \xi_0 + \xi'$, $\tilde{\eta} = \eta_0 + \eta'$ and $\tilde{\mathscr{C}} = 0 + \mathscr{C}'$, where $h' = \xi' - \eta'$. An expansion of equations (1a, 1b, 1c) in ν up to $O(\nu^2)$ yields the following results. For zeroth order, equations (1a) and (1c) yield

$$C_f U^2 = gHI; \quad UH = q_w, \tag{2}$$

where q_w is constant water discharge per unit width; (1b) vanishes. Equations (1a) and (1c) do not contribute at $O(\nu)$; (1b) yields

$$U^2\mathscr{C}' = g\frac{\partial \xi'}{\partial \tilde{n}}. \tag{3a}$$

Equation (1b) does not contribute at $O(\nu^2)$; (1a) and (1c) yield, respectively,

$$U\frac{\partial u'}{\partial \tilde{s}} = -g\frac{\partial \xi'}{\partial \tilde{s}} - C_f\frac{U^2}{H}\left(2\frac{u'}{U} - \frac{\xi'}{H} + \frac{\eta'}{H}\right), \tag{3b}$$

$$H\left(\frac{\partial u'}{\partial \tilde{s}} + \frac{\partial v'}{\partial \tilde{n}}\right) + U\frac{\partial h'}{\partial \tilde{s}} = 0. \tag{3c}$$

The reach-averaged values of U, H, and I may be taken to be spatially constant, but must vary slowly in time. As bends grow, the channel centreline arc-length over one Cartesian wavelength $\int_0^\lambda \gamma^{-1} d\tilde{x}$, where $\gamma = [1 + (\partial\tilde{y}/\partial\tilde{x})^2]^{-\frac{1}{2}}$, must increase in time. If the stream is to experience neither aggradation nor degradation in its valley, the elevation drop Δz over one wavelength must be constant in time. Reach-averaged channel slope is then

$$I = \frac{\Delta z}{\int_0^\lambda \gamma^{-1} d\tilde{x}} = \frac{I_0}{\overline{\gamma^{-1}}}, \tag{4}$$

where $I_0 = \Delta z/\lambda$ is valley slope, $\gamma = \cos\theta$, and the overbar denotes averaging over one wavelength. Thus channel slope must decrease as sinuosity increases in time, and

$I = I(t)$. It then follows from (2) that U and H must vary in time as well. The effect is embodied in the geometric nonlinearity of the expression for arc-length in $\tilde{y}$.

Equation (3*a*) integrates to yield

$$\xi' = \frac{1}{g}\mathscr{C}'U^2\tilde{n}. \tag{5}$$

This must be supplemented by a relation for η'. The St Venant equations do not allow for a treatment of secondary flow in bends, and the resulting lateral variation in bed elevation. However, Engelund (1974), Ikeda (1975), Kikkawa, Ikeda & Kitagawa (1976), and Zimmerman & Kennedy (1978) have analysed this problem with three-dimensional treatments of the alluvial case. Their result to $O(\nu)$ is

$$\frac{\eta'}{H} = -AC'\tilde{n}, \tag{6}$$

where A is an $O(1)$ parameter. Examination of the governing equations indicates that this result is not changed at $O(\nu^2)$. Engelund (1974) used this fact and equations (3*a*) and (3*b*) (equations (47) and (52) in his analysis) to obtain an $O(\nu^2)$ description of tangential velocity variation u' and bed topography that exhibits good agreement with the experimental data of Hooke (1975).

Engelund suggested a constant value of A of about four. The theories of Kikkawa *et al.* (1976) and Zimmerman & Kennedy (1978) predict similar values, but both theories predict that A should increase with U. Herein the problem of specifying this variation is avoided by simply using an average value of A based on field data. An analysis of 45 bends of ten alluvial rivers in Japan based on data collected by Suga (1963) suggests an average value of 2·89, although the data show much scatter. This value is used herein for the alluvial case.

In order to evaluate bank erosion, it will prove useful to determine near-bank velocity. An equation for $u_b' = (u')_{\tilde{n}=b}$ can be developed by substituting (5) and (6) into (3*b*) and evaluating at $\tilde{n} = b$; it is found that

$$U\frac{\partial u_b'}{\partial \tilde{s}} + 2\frac{U}{H}C_f u_b' = b\left[-U^2\frac{\partial \mathscr{C}'}{\partial \tilde{s}} + C_f\mathscr{C}'\left(\frac{U^4}{gH^2} + A\frac{U^2}{H}\right)\right]. \tag{7}$$

Relations (2) and (7) are now made dimensionless. The scales used are U_0 and H_0, the values that U and H would take in a graded (other than meandering tendencies) perfectly straight channel with width equal to $2b$ and channel slope equal to the valley slope I_0. Let $\tilde{x} = H_0 x$, $\tilde{y} = H_0 y$, $U = U_0\chi(t)$, and $H = H_0\Xi(t)$. Then

$$\gamma(t) = \cos\theta = \left\{1 + \left(\frac{\partial y}{\partial x}\right)^2\right\}^{-\frac{1}{2}}, \tag{8}$$

and from (2) and (4)

$$\chi(t) = [\overline{\gamma^{-1}}]^{-\frac{1}{3}}, \quad \Xi(t) = \chi^{-1}. \tag{9}$$

In addition, where $u_b' = U_0 u$, $\mathscr{C}' = H_0^{-1}\mathscr{C}$, $\tilde{s} = H_0 s$ and $\tilde{n} = H_0 n$, (7) reduces with the aid of (9) to

$$\frac{\partial u}{\partial s} + 2\chi C_f u = b^*\left[-\chi\frac{\partial \mathscr{C}}{\partial s} + C_f\mathscr{C}(F^2\chi^5 + A\chi^2)\right], \tag{10}$$

where $b^* = b/H_0$ and $F = U_0/(gH_0)^{\frac{1}{2}}$.

The reason for expressing (7), and by implication (10), in terms of 'north' bank

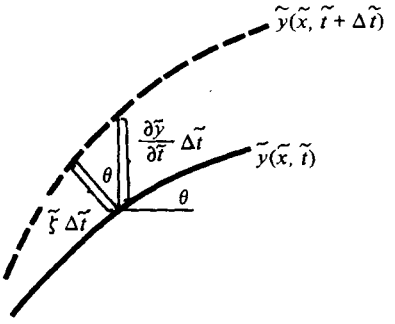

FIGURE 3. Diagram for derivation of the equation of bank erosion, (11).

velocity (at $\tilde{n} = b$; see figure 2) is related to the equation of bank erosion developed in the next section.

3. Equation of bank erosion

Let $\tilde{\zeta}$ be the rate of normal bank erosion in, say, metres/year of the 'north' bank in figure 2. If ν is sufficiently small geometrical considerations dictate that

$$\gamma \frac{\partial \tilde{y}}{\partial \tilde{t}} = \tilde{\zeta}, \tag{11}$$

where $\gamma = \cos\theta$ (figure 3). This equation describes 'north' bank erosion (or deposition if $\tilde{\zeta}$ is negative). The condition of constant normal width assures that in the alluvial case erosion of the 'north' bank corresponds to equal deposition at the 'south' bank. Equation (11) can also be applied to incising bends, the location of the 'south' bank being again determined by the condition of constant width, in this case maintained by a balance between lateral erosion and vertical incision.

Now $\tilde{\zeta}$ is assumed to be a function of tangential flow velocity near the 'north' bank $\tilde{u}(\tilde{s}, \tilde{n})|_{\tilde{n}=b} = U + u'(\tilde{s}, b)$. Its functional form is estimated as

$$\tilde{\zeta} \equiv \tilde{\zeta}(U) + \left.\frac{d\tilde{\zeta}}{d\tilde{u}}\right|_U u'(\tilde{s}, b) \equiv \tilde{\zeta}(U) + E(U)u'(\tilde{s}, b), \tag{12}$$

where $E(U) = [d\tilde{\zeta}/d\tilde{u}]|_U$ is a positive coefficient of bank erosion. In the above $\tilde{\zeta}(U)$ is assumed to vanish. This latter condition implies that reach-averaged river width is in grade, and that only local variation from reach-averaged values can cause bank migration. Thus for the alluvial case, (12) implies that the 'north' bank erodes where near-bank velocities are above the reach-averaged value ($u'(\tilde{s}, b) > 0$), with consequent deposition on the adjacent 'south' bank, and vice versa if $u'(\tilde{s}, b) < 0$. A similar interpretation applies to the incised case. Sawai & Ashida (1979) have developed methods for estimating E for cohesive material.

Relations (11) and (12) reduce to the dimensionless form

$$\gamma\, \partial y/\partial t = E(\chi)u, \quad \text{where} \quad t = \tilde{t}U_0/H_0. \tag{13}$$

The nonlinear analysis of Part 2 requires that an assumption be made as regards the dependence of E on reach-averaged velocity U (i.e. χ). Consider two adjacent reaches, one with a slightly higher channel slope and therefore a swifter reach-averaged flow

velocity than the other. The swifter flow velocity suggests a higher rate of bank erosion at the outside of a bend (and thus a higher rate of deposition at the inside). If this is correct, then $E(\chi)$ can be taken to be a monotonically increasing function of χ. This assumption is reasonable and is made herein; however it should be noted that the problem is more complex than this, in that E might also depend on the variation of sediment load available for deposition. A consequence of the assumption is

$$\frac{1}{E}\frac{dE}{d\chi}\bigg|_1 \equiv e > 0.$$

Thus, if the magnitude of $\chi - 1$ is not large, a Taylor expansion of E about $\chi = 1$ yields

$$E(\chi) = E_0[1 + e(\chi - 1)], \tag{14}$$

where $E_0 = E(1)$.

Fortunately, the parameter e plays no role in the linear theory.

4. The bend equation

The transformations from intrinsic to Cartesian co-ordinates dictate that, in dimensionless form,

$$\frac{\partial}{\partial s} = \gamma\frac{\partial}{\partial x}, \quad \mathscr{C} = -\gamma^3\frac{\partial^2 y}{\partial x^2}.$$

Equations (10), (13) and (14) reduce with these to yield the nonlinear bend equation expressed in Cartesian co-ordinates:

$$\frac{\partial}{\partial x}\gamma\frac{\partial y}{\partial t} + 2\chi C_f\frac{\partial y}{\partial t} = [1 + e(\chi - 1)]\left[\chi\frac{\partial}{\partial x}\gamma^3\frac{\partial^2 y}{\partial x^2} - C_f(F^2\chi^5 + A\chi^2)\gamma^2\frac{\partial^2 y}{\partial x^2}\right]. \tag{15}$$

In the above the constant $E_0 b^*$ has been absorbed by the transformation $E_0 b^* t \to t$. χ and γ are nonlinearly coupled to y via equations (8) and (9).

The term $\partial y/\partial x$ can be estimated as $2\pi y_0/\lambda$, where y_0 and λ, are dimensional quantities. Defining dimensionless amplitude and wavenumber $\epsilon = y_0/H_0$ and $k = 2\pi H_0/\lambda$, respectively, the following order-of-magnitude estimate can be obtained:

$$(\partial y/\partial x)^2 \sim \delta_0^2,$$

where $\delta_0 = k\epsilon$. In the limit of small δ_0, corresponding to small-amplitude bends, then, $\chi \cong 1$, $\gamma \cong 1$ and (15) linearizes to

$$\frac{\partial^2 y}{\partial x\,\partial t} + 2C_f\frac{\partial y}{\partial t} = \frac{\partial^3 y}{\partial x^3} - C_f(A + F^2)\frac{\partial^2 y}{\partial x^2}. \tag{16}$$

In the above both amplitude-dependent geometric nonlinearities and curvature-dependent dynamic nonlinearities have been removed.

5. Linear stability analysis

For the purpose of studying the stability of straight banks, the bank geometry fluctuation

$$y = \epsilon\, e^{\alpha_0 t}\cos(kx - \omega_0 t) \tag{17}$$

is considered. In the above α_0 is dimensionless amplitude growth-rate and ω_0 is dimensionless migration frequency; $c_0 = \omega_0/k$ is downstream bend migration speed.

The subscript zero refers to the fact that these values are to be obtained from a linear theory. In the companion paper they are expanded in δ_0 to obtain expressions of the general type $\alpha = \alpha_0 + \epsilon^2\alpha_2 + \ldots$. Insertion of (17) into (16) yields the dispersion relations

$$\omega_0 = \frac{C_f k^3(2+A+F^2)}{k^2+4C_f^2}, \quad c_0 = \frac{\omega_0}{k}, \quad \alpha_0 = \frac{2C_f^2(A+F^2)k^2 - k^4}{k^2+4C_f^2}. \tag{18}$$

It is seen that instability occurs if

$$k < \sqrt{2}\, C_f (A+F^2)^{\frac{1}{2}}, \tag{19}$$

where the right-hand-side corresponds to the wavenumber of neutral instability.

The wavenumber k_{OM} at which instability is maximized can be obtained from the condition $\partial\alpha_0/\partial k = 0$; it is found to be

$$k_{OM} = \beta C_f, \tag{20}$$

where

$$\beta^2 = 4\{1 + \tfrac{1}{2}(A+F^2)\}^{\frac{1}{2}} - 4. \tag{21}$$

At $k = k_{OM}$, α_0 and ω_0 are found to take the values

$$\alpha_{OM} = \tfrac{1}{4}\beta^2 k_{OM}^2, \tag{22}$$

$$\omega_{OM} = \tfrac{1}{2}k_{OM}^2\beta(1+\tfrac{1}{4}\beta^2). \tag{23}$$

Two cases are of particular interest. Nearly all natural alluvial meandering streams at flood stage satisfy the condition $F^2 \ll A$ where A is approximated by 2·89 as previously mentioned. In the alluvial case, then, $\beta \cong 1{\cdot}50$ and the approximate forms

$$k_{OM} = 1{\cdot}50 C_f, \quad \alpha_{OM} = 0{\cdot}564 k_{OM}^2, \quad \omega_{OM} = 1{\cdot}17 k_{OM}^2 \tag{24a, b, c}$$

are obtained. Downstream migration speed at maximum instability is $c_{OM} = \omega_{OM}/k_{OM}$, or

$$c_{OM} = 1{\cdot}17 k_{OM}. \tag{25}$$

The other case of interest is that of a laterally flat bed ($A = 0$). For this case, which is later shown to apply to some cases of incised meandering,

$$k_{OM} = \beta^* C_f, \quad \alpha_{OM} = \tfrac{1}{4}\beta^{*2}k_{OM}^2, \quad \omega_{OM} = \tfrac{1}{2}\beta^* k_{OM}^2(1+\tfrac{1}{4}\beta^{*2}) \tag{26a, b, c}$$

and also

$$c_{OM} = \tfrac{1}{2}\beta^* k_{OM}(1+\tfrac{1}{4}\beta^{*2}), \tag{27}$$

where $\beta^* = 2\{-1 + (1+\frac{1}{2}F^2)^{\frac{1}{2}}\}^{\frac{1}{2}}$. For the case of alluvial rivers, $\frac{1}{2}F^2$ is generally small, so that $\beta^* \cong F$ and, for example,

$$k_{OM} \cong C_f F. \tag{28}$$

In general, for $A \geqslant 0$ a range of wavenumbers for which bends grow in amplitude is seen to exist. From (18) it is seen that bends always migrate downstream, whether stable or unstable, and regardless of Froude number. This result represents a correction of the heuristic conclusion reached in Ikeda *et al.* (1976) that stable bends migrate upstream. In addition equation (24*a*) predicts meander wavelengths that differ considerably from the result $k_{OM} = \sqrt{\frac{2}{3}}\, C_f F$ obtained therein.

6. Discussion

The relation of the bend theory to bar theories merits some discussion.

The bend theory incorporates the occurrence of point bars on the inside of each bend via (6); point bar location is determined by curvature. The location of alternate bars in straight-channel bar theories is arbitrary. The two types of bars, and thus the two stability mechanisms, are fundamentally different. Straight-channel bar theories drop curvature in (1*b*) but retain inertial and friction terms involving $\tilde{v}$, which are required for bar instability; the situation is reversed for the bend theory. A more general three-dimensional formulation retaining all linearized terms in a relation analogous to (1*b*) would thus be likely to exhibit a dual instability mechanism.

In order to clarify the range of influence of each mechanism, it is useful to consider a meandering channel that has developed point bars on the inside of the bends. Into this channel the further perturbation of an alternate-bar pattern with bed elevation amplitude η_a and arbitrary location and wavelength λ_a, is introduced. The tangential velocity perturbation u' due to bends and alternate bars can be estimated as $U(b/r_0)$ and $U(\eta_a/H)$ respectively; according to (1*c*) v' can be estimated as

$$\frac{b}{r_0}u' \sim \left(\frac{b}{r_0}\right)^2 U \quad \text{and} \quad \frac{b}{\lambda_a}u' \sim \frac{b}{\lambda_a}\frac{\eta_a}{H}U$$

respectively. The ratio of inertial to curvature terms in (1*b*) can thus be shown to scale as

$$\text{ratio} \sim \left(\frac{b}{r_0}\right)^3 \quad \text{and} \quad \text{ratio} \sim \left(\frac{br_0}{\lambda_a^2}\right)\frac{\eta_a}{H}$$

for bends and alternate bars respectively. For the latter case, λ_a may be held constant as curvature becomes arbitrarily small ($r_0 \to \infty$); the ratio becomes large and the straight-channel bar approximation in (1*b*) is obtained. For the former case point-bar spacing is controlled by curvature; for sufficiently small curvature the ratio becomes small and the bend approximation of (1*b*) is obtained.

Thus the bend approximation may require modification in meandering channels that exhibit bar spacings different from that imposed by curvature. Kinoshita (1957) has observed the bar structure in a large number of alluvial streams; he notes that in bends of small or moderate curvature each bend contains only one point bar, whereas in tortuous bends several alternate bars may be superimposed over a primary point bar. Likewise, Hooke's (1975) experiments in a channel of moderate curvature exhibit only point bars; this suggests that a range of small but non-vanishing curvature exists for which the bend mechanism is the more important of the two. However it is interesting that both mechanisms seem to operate at similar scales, as shown in the following section.

7. Comparison with data

The wavelength of maximum instability of a linear stability analysis of meandering is generally thought to provide a crude estimate of the wavelength of the finite-amplitude meanders realized in nature. This assumption is used herein, even though a complete justification is lacking.

It is useful to compare the results of bend stability in this regard with those of

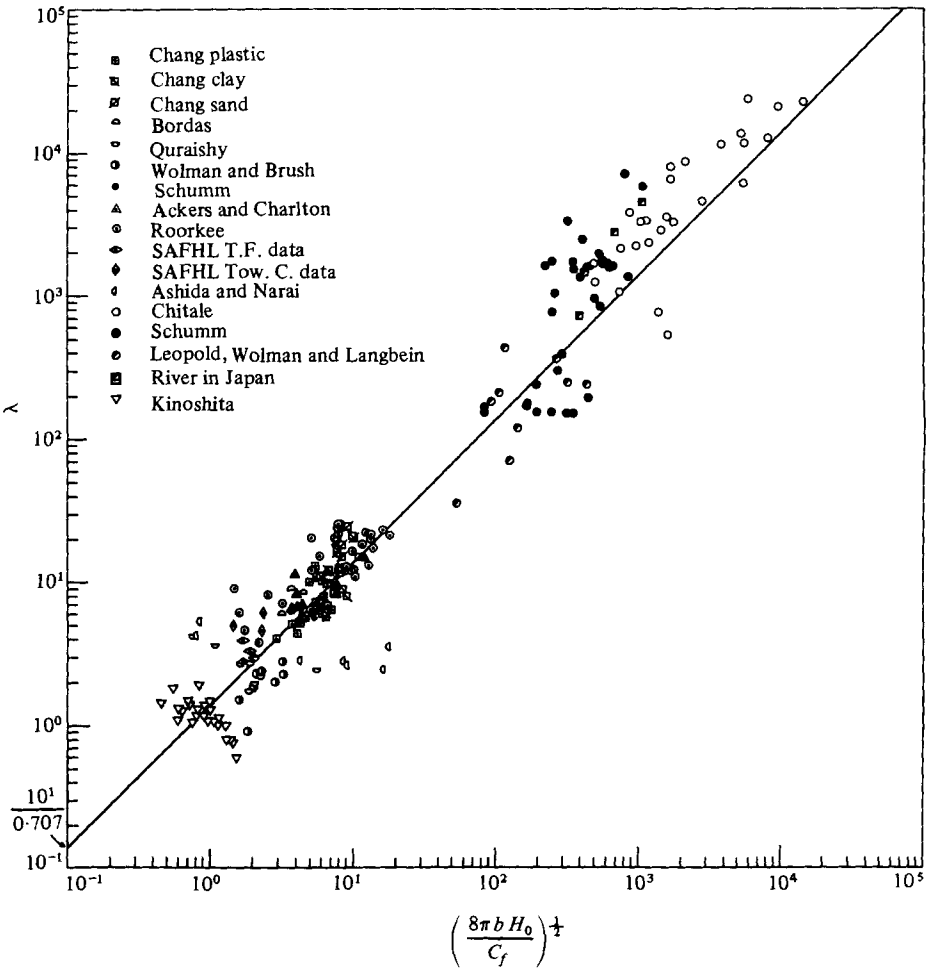

FIGURE 4. Test of equation (30) for alluvial data; the units are metres.

alternate bar theories. To this end several results of Parker (1975) for incisional alternate bars and of Parker (1976) for alluvial alternate bars are quoted. Since $k_{OM} = 2\pi H_0/\lambda$ is the wavenumber of maximum instability and $l = \pi H_0/2b$, the results are

$$k_{OM}^2 = F^{-2}(k_{OM}^2 + l^2)^{\frac{1}{2}} \tanh (k_{OM}^2 + l^2)^{\frac{1}{2}}, \tag{29}$$

and

$$k_{OM} = aC_f^{\frac{1}{2}} l^{\frac{1}{2}} \tag{30}$$

for the incisional and alluvial cases respectively; a is an $O(1)$ function of Froude number which approximates to a constant for $F \ll 1$. The constant depends on the choice of load and resistance relations. Parker & Anderson (1975) have found that (30) provides reasonable estimates for laboratory experiments if a is approximated by a constant; the choice $a \cong 0{\cdot}707$ is suggested by data.

It is necessary to choose some representative 'dominant' discharge in order to analyse field data from alluvial channels. Herein the mean annual flood is used for all cases in which it is available; bankfull discharge is used otherwise.

Equation (30) of alluvial bar theory and (24a) of alluvial bend theory are tested

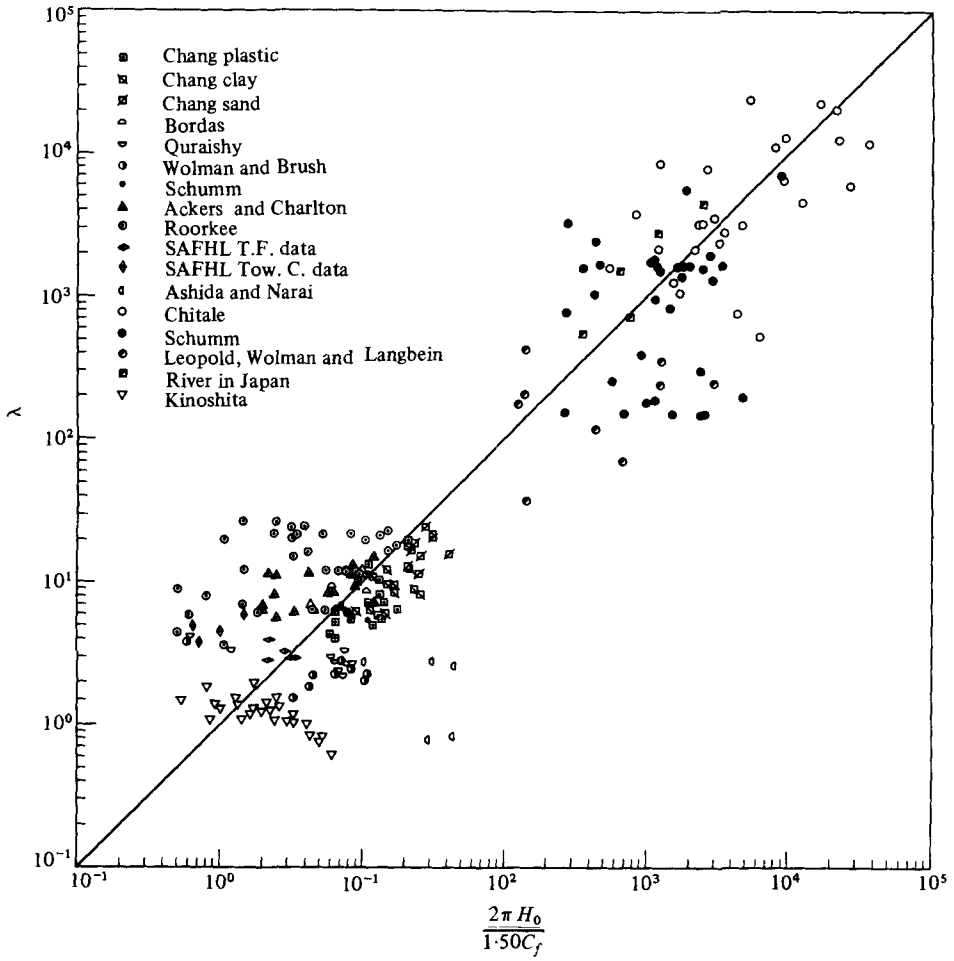

FIGURE 5. Test of equation (24*a*) for alluvial data; the units are metres.

against 158 sets of data from alluvial river trays and 73 sets from natural alluvial rivers in figures 4 and 5, respectively. The plots are in terms of observed (λ) and predicted (λ_{pred}) wavelength rather than wavenumber. Both relations provide rough agreement. The data scatter less about the prediction of alluvial bar theory. On the other hand equation (24*a*) of bend theory contains no adjustable constant to be fitted to the data, whereas such a constant appears in (30). It may be that the scatter in figure 5 would be reduced if measured values of A for each stream were used instead of the 'typical' value of 2·89.

A point of significance is that the meander wavelength predicted by the bend and alluvial bar theories are seen to be the same order of magnitude.

The incised bar theory of Parker (1975) indicates instability only for supercritical flows; the bars do not migrate downstream. No assumption in the bend theory restricts it to the alluvial case. Thus (20) and (21) should apply to incised bends for an appropriate choice of A. Instability can occur for any Froude number; the bends migrate downstream. These features suggest the possibility of distinguishing between two types. Ashida & Sawai (1977) have observed the formation of incised rill meanders in

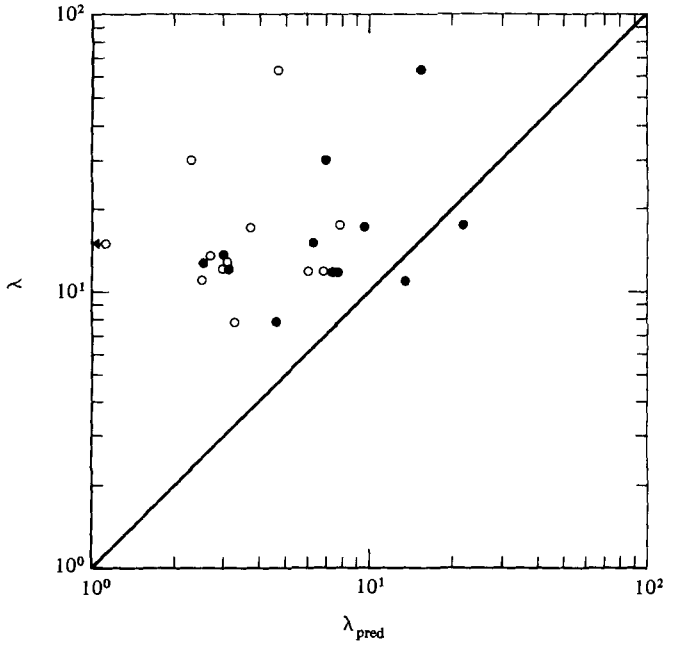

FIGURE 6. Test of equations (26*a*) (dark circles) and (29) (open circles) for data on incised rill meanders; λ_{pred} denotes the predicted wavelength. The units are centimetres.

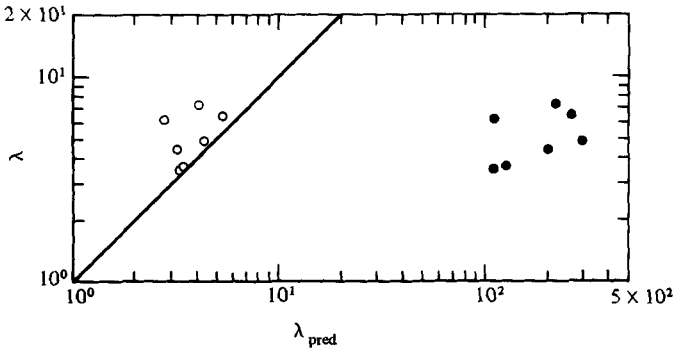

FIGURE 7. Test of equations (26*a*) (dark circles) and (29) (open circles) for data on supraglacial meltwater stream meandering; λ_{pred} denotes the predicted wavelength. The units are metres.

a cohesive sand–clay medium in the laboratory. Of eleven data sets reported therein, all but one are supercritical. No definite lateral bed inclination was observed; in light of this A was set equal to zero and (26*a*) of the bend theory was used along with (29) of the bar theory to estimate meander wavelength. The results are shown in figure 6; the bend theory appears to predict the wavelength somewhat better than the bar theory even though the flows are generally supercritical. One more factor that suggests that these meanders are due to bend instability is the direction of migration. In some runs irregularities associated with smaller-scale upstream-migrating two-dimensional erosional bedforms render any orderly bend progression difficult to perceive. In other runs, however, a distinct pattern of downstream bend migration was observed, whereas a distinct pattern of upstream-migrating bends was observed for no run.

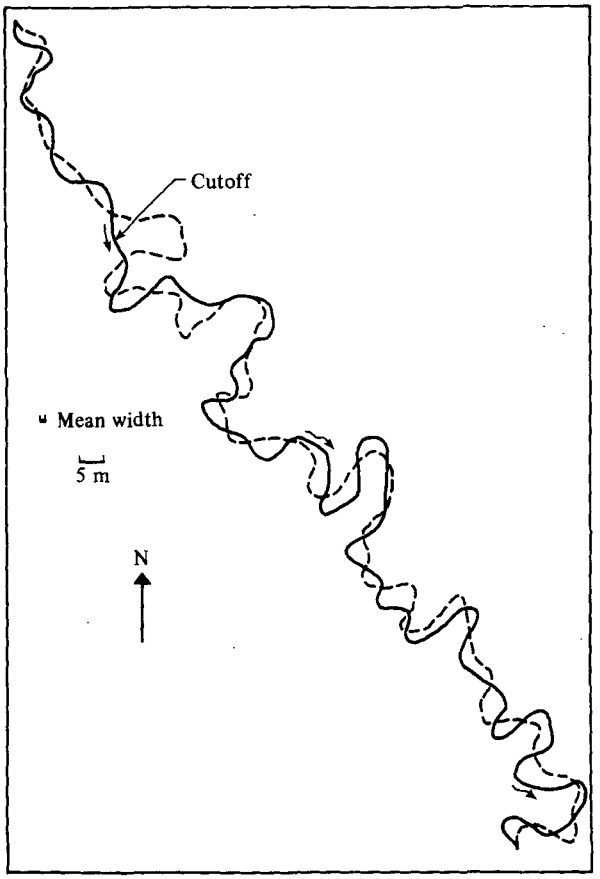

FIGURE 8. Planform centreline of a reach of Gardner's Gut, New Zealand, an incised cave stream. The solid line denotes the present centreline of the stream, and the dashed line denotes the centreline two metres above the stream. From Smart (1977).

The supraglacial meandering meltwater streams described by Dahlin (1974) and analysed by Parker (1975) present another type of incised meander. The data, consisting of seven sets from supraglacial streams on Baffin Island, do not include slope; nevertheless C_f could be estimated from known depths, velocities and water temperatures, and the Kármán–Prandtl resistance relation for smooth boundaries. For want of information about A, equation (26a) was utilized to test the bend theory, along with (29) for the bar theory. The results, shown in figure 7, suggest that these incised meanders have their origin in the bar theory. No $O(1)$ choice of A could improve the poor predictability of the bend theory much in this case.

8. Unified interpretation of the growth of meanders

Figures 4 and 5 indicate that alluvial bar and bend instability act at characteristic wavelengths that are of the same order of magnitude. This justifies the assumption, implicit in previous studies, that alternate bar formation should be followed by the formation of a truly sinuous channel with bends exhibiting superelevation and secondary flow, such that each bend contains one alternate bar.

In two cases of incised meandering analysed, those of model channels in cohesive material and supraglacial meltwater streams, it is seen that the two mechanisms operate at differing scales. Figures 6 and 7 suggest that bend instability is responsible for the former, and bar instability for the latter.

The analysis provides clues in other cases as well. In figure 8 the planform of the bottom of a cave stream incised in limestone is shown with the planform two metres above. The direct evidence of downstream migration suggests that the bend instability is responsible for the meanders (Smart 1977).

A final point of interest is the observation that incised field meanders often have larger wavelengths than alluvial meanders (e.g. Hack 1965). The condition $\frac{1}{2}F^2 \ll 1$ is probably satisfied in many of the larger of such streams. If the surmise $A = 0$ for incised meanders is correct, it is seen from equations (24a) and (28) that the ratio of incised wavelength to alluvial wavelength where flow conditions and channel geometry are the same is given by the ratio $\beta^2/F^2 = 2{\cdot}25F^{-2}$, so that incised meanders would have a larger wavelength. The data of Ashida & Sawai (1977) on incised rill meanders support the choice $A = 0$, and Smart (personal communication) has observed no systematic variation in lateral bed elevation at the bed apexes of incised cave meanders, again suggesting the choice $A = 0$. Evidence to the same effect can be found in the voluminous set of cave surveys contained in Tratman (1969).

REFERENCES

Adachi, S. 1967 A theory of stability of streams. *Proc. 12th Congr. IAHR*, vol. 1, pp. 338–343.

Ashida, K. & Sawai, K. 1977 A study on the stream formation process on a bare slope (3). *Annuals, Disaster Prevention Research Institute, Kyoto University*, no. 20B–2 (in Japanese).

Callander, R. A. 1969 Instability and river channels. *J. Fluid Mech.* **36**, 365–480.

Dahlin, B. 1974 A contribution to the study of meandering. M.Sc. Thesis, Dept. of Geology, Univ. of Minnesota, Minneapolis, Minn., U.S.A.

Engelund, F. 1974 Flow and bed topography in channel bends. *J. Hydraul. Div., Proc. ASCE*, **100**, 1631–1648.

Engelund, F. & Skovgaard, O. 1973 On the origin of meandering and braiding in alluvial streams. *J. Fluid Mech.* **57**, 289–302.

Fredsoe, J. 1978 Meandering and braiding of rivers. *J. Fluid Mech.* **84**, 607–624.

Hack, J. T. 1965 Post-glacial drainage evolution and stream geometry in the Ontonagon area. Michigan, *U.S. Geol. Surv. Prof. Paper* no. 504–13.

Hansen, E. 1967 The formation of meanders as a stability problem. *Hydraul. Lab., Tech. Univ. of Denmark, Basic Res. Prog. Rep.*, no. 13.

Hayashi, T. 1970 The formation of meanders in rivers. *Proc. Japan Soc. Civ. Engrs*, no. 180 (in Japanese).

Hayashi, T. & Ozaki, Y. 1976 On the meander wavelength from the view point of bar instability theory. *Proc. 20th Annual Meeting, Hydraul., Japan Soc. Civ. Engrs*, pp. 89–96 (in Japanese).

Hooke, R. le B. 1975 Distribution of sediment transport and shear stress in a meander bend. *Journal of Geology* V, **83**, 543–565.

Ikeda, S. 1975 On secondary flow and bed profile in alluvial curved open channel. *Proc. 16th Congr. IAHR*, vol. 2, pp. 105–112.

Ikeda, S., Hino, M. & Kikkawa, H. 1976 Theoretical study on the free meandering of rivers. *Proc. Japan Soc. Civ. Engrs*, no. 255, pp. 63–73 (in Japanese).

Ikeda, S. 1978 Roles of secondary flow in the formation of channel geometry. *Proc. U.S.–Japan Seminar on Sedimentation*, 1978.

Kikkawa, H., Ikeda, S. & Kitagawa, A. 1976 Flow and bed topography in curved open channels. *J. Hydraul. Div., Proc. ASCE*, **102**.

KINOSHITA, R. 1957 Formation of dunes on river bed. *Trans. Japan Soc. Civ. Engrs.*, no. 42 (in Japanese).

LEOPOLD, L. B., WOLMAN, M. G. & MILLER, J. P. 1964 *Fluvial processes in Geomorphology.* Freeman.

PARKER, G. 1975 Meandering of supraglacial melt streams. *Water Resources Res.* **11**, 551–552.

PARKER, G. 1976 On the cause and characteristic scales of meandering and braiding in rivers. *J. Fluid Mech.* **76**, 457–480.

PARKER, G. & ANDERSON, A. G. 1975 Modelling of meandering and braiding in rivers. *Proc. ASCE Modelling Symposium* 1975, San Francisco, pp. 575–591.

PARKER, G., SAWAI, K. & IKEDA, S. 1982 Bend theory of river meanders. Part 2. Nonlinear deformation of finite-amplitude bends. *J. Fluid Mech.* (to be published).

PONCE, V. M. & MAHMOOD, K. 1976 Meandering thalwegs in straight alluvial channels. *Proc. ASCE Rivers Conference* 1976, Fort Collins, Colorado.

SAWAI, K. & ASHIDA, K. 1979 A test method of soil erodibility by means of the rotating cylinder. *Annuals, Disaster Prevention Research Institute, Kyoto University*, no. 22B–2 (in Japanese).

SCHUMM, S. A. 1969 River metamorphosis. *J. Hydraul. Div., Proc. ASCE* **96**, 201–222.

SMART, C. 1977 A statistical analysis of cave meanders. M.Sc. thesis, Dept. of Geography, University of Alberta, Edmonton, Alberta, Canada.

SUGA, K. 1963 On local scour at river bends. *Tech. Memo Public Works Res. Inst., Min. of Const. Japan*, vol. 5, no. 4 (in Japanese).

SUKEGAWA, N. 1970 Conditions for the occurrence of river meanders. *J. Faculty of Eng., Univ. of Tokyo*, vol. 30, pp. 289–306.

TRATMAN, E. K. 1969 *The Caves of North-West Clare, Ireland.* David and Charles: Newton Abbot, London.

ZIMMERMAN, C. & KENNEDY, J. F. 1978 Transverse bed slopes in curved alluvial streams. *J. Hydraul. Div., Proc. ASCE*, **104**, 33–48.